Accelerated weathering affects the chemical and physical properties of marine antifouling paint microplastics and their identification by ATR-FTIR spectroscopy

Simon, Marta; Vianello, Alvise; Shashoua, Yvonne ; Vollertsen, Jes

Published in:
Chemosphere

DOI (link to publication from Publisher):
10.1016/j.chemosphere.2021.129749

Publication date:
2021

Document Version
Publisher's PDF, also known as Version of record

Chemosphere 274 (2021) 129749

Contents lists available at ScienceDirect

Chemosphere

journal homepage: www.elsevier.com/locate/chemosphere

Accelerated weathering affects the chemical and physical properties of marine antifouling paint microplastics and their identification by ATR-FTIR spectroscopy

Márta Simon [a, *], Alvise Vianello [a], Yvonne Shashoua [b], Jes Vollertsen [a]

[a] Department of the Built Environment, Aalborg University, Thomas Manns Vej 23, Aalborg, DK, 9220, Denmark
[b] Environmental Archaeology and Materials Science, National Museum of Denmark, IC Modewegsvej-Brede, Kongens Lyngby, DK, 2800, Denmark

HIGHLIGHTS

- Weathering impairs the binder structure of antifouling paint microparticles.
- Impaired binder structure leads to increased heavy metal release.
- Weathering hinders the identification of paints based on their infrared spectra.

GRAPHICAL ABSTRACT

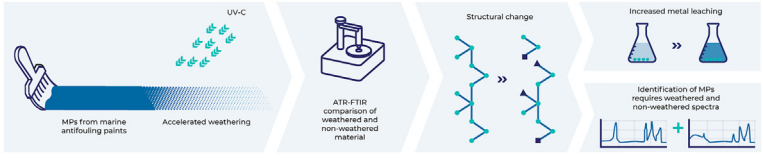

ARTICLE INFO

Article history:
Received 25 November 2020
Received in revised form
14 January 2021
Accepted 18 January 2021
Available online 28 January 2021

Handling Editor: Michael Bank

Keywords:
Antifouling paint
Weathering
Metal leaching
Infrared spectroscopy

ABSTRACT

Microplastics prepared from commercial marine antifouling paints were weathered by UV-C irradiation representing between 25 and 101 days of real-time, outdoor exposure. Attenuated Total Reflection Fourier Transform Infrared (ATR-FTIR) spectroscopy of the degraded paint particles showed that weathering induced chemical changes in the material, including the release of volatile components and the formation of hydrophilic groups. The chemical changes and increased reactivity of the paint binder were associated with alterations in their physical properties and increased leaching of metals in freshwater conditions. Changes in the spectra obtained from weathered paint samples reduced their match with spectra of unaged materials, resulting in a poorer similarity index, the Score when using automatic identification tools for microplastics. The results suggest that spectra of weathered, as well as pristine paint microplastics, should be consulted when applying analytical pipelines to identify microplastics extracted from natural matrices.

1. Introduction

Plastic litter in the environment is exposed to various impacts, such as UV-radiation, fluctuating temperatures, mechanical friction and microbial activity, that weather their material (Andrady, 2017). These processes change both the material's physical and chemical properties, resulting in the generation of small plastic particles, called secondary microplastics (MPs) (Andrady, 2011a; Browne et al., 2007). Since these MPs are further exposed to weathering impacts, they can undergo additional physicochemical changes. UV-exposure is a primary weathering factor, because its high energy weakens polymer structures, leaving them vulnerable to particle abrasion, changes in crystallinity and the formation of new hydrophilic functional groups in the polymer (Bejgarn et al., 2015; Hammer et al., 2012; Rabek, 1990). The resulting impaired polymeric structure, increased surface area and hydrophilicity of the MPs can facilitate the release of compounds that are not chemically bound to the polymer, such as additives and residual substances from the production process (Bejgarn et al., 2015; Hahladakis et al.,

* Corresponding author.
E-mail address: h.marta.simon@gmail.com (M. Simon).

https://doi.org/10.1016/j.chemosphere.2021.129749

2018; Hermabessiere et al., 2017). Consequently, weathering can increase the threat that plastic litter and MPs pose to the environment due to the mobilised compounds' potentially toxic nature (Hermabessiere et al., 2017; Lithner et al., 2011).

The definition of microplastics is broad and covers microparticles of a wide range of polymeric materials. Rubbers, composite materials and paints with polymeric binders are for example included under the umbrella of 'microplastics' (AnnexRestr, 2019; Hartmann et al., 2019). Of these, microparticles of antifouling paints can be of special concern as antifouling coatings are designed to release heavy metals and biocidal compounds to control the growth of a variety of organisms (Yebra et al., 2004; Jartun and Pettersen, 2010). Studies have reported such particles in high numbers, for example at boat maintenance sites where the heavy metal concentrations in soil and road dust samples in the vicinity were elevated and the concentration of organotin compounds at longer distances from the source was associated with their presence (Turner, 2010; Turner et al., 2009; Decelis and Vella, 2007). The dispersion of antifouling paint particles potentially affects a wide range of organisms in marine, freshwater and terrestrial habitats.

The present study explores the effect of UV-exposure on the impact of antifouling paint microparticles by employing accelerated weathering. It investigates the influence of weathering on particle size and metal release in freshwater conditions and seeks to link the chemical alterations induced in the paint measured using Attenuated Total Reflection-Fourier-transform infrared (ATR-FTIR) spectroscopy to the observed changes of physical properties. Furthermore, it assesses the effect of weathering on the identification of paint materials.

2. Materials and methods

We identified the main organic and inorganic components and followed the UV-induced chemical changes in the paint materials with ATR-FTIR spectroscopy. We examined the sizes of the non-exposed and UV-exposed microparticles using a flow imaging particle analyzer and a stereomicroscope. We evaluated the release of metals from the paint microparticles with inductively coupled plasma - optical emission spectrometry (ICP-OES).

2.1. Materials

We prepared microplastics from paint films of six common commercial marine antifouling paints after application according to the manufacturers' instructions. One layer of Hempel's Underwater Primer 26030 and two layers of paint were brushed onto bakery release paper for easy removal of the dry paint with 24 h drying time between each coat. The properties of the studied paints are summarised in Table 1. After drying, paint films were cut into flakes (approximately 5 × 5 cm) and some were ground into particles under liquid nitrogen using a porcelain pestle and mortar. The particles were dry sieved through 500 and 20 μm stainless steel meshes to obtain microparticles in size range of 20–500 μm. Although dry-sieving generally results in poorer particle separation than wet-sieving, it was selected to minimise the risk of metal leaching during the process. The microparticles of the paints containing both zinc oxide and copper(I) oxide were mixed in equal proportions for the leaching experiments and we refer to the mixture hereafter as paint mix. We refer further to the individual paints as Cruiser, Nautical, Racing, Seajet, Yachting and Alusafe.

2.2. Accelerated weathering

Individual paint flakes and microparticles were weathered in a BS-02 irradiation chamber from Opsytech Dr. Gröbel GmbH, Germany. The chamber was equipped with eight UV-C lamps, each delivered 10 mW cm^{-2} irradiance at 253 nm. We determined exposure times of paint microparticles by initially irradiating large paint flakes for between one and four weeks. The solar equivalence was calculated by comparing the number of photons that the UV-C lamps emitted with the estimated amount of photons in yearly average sunlight in Denmark. We quantified the photons according to equation (1)

$$N = \frac{E}{h\frac{c}{\lambda}} \quad (1)$$

E is the energy of N photons in J, h is the Planck's constant (6.63 10^{-34} J s), c is the speed of light (3 10^{8} m s^{-1}) and λ is the wavelength of the light (m) (Wypych, 2015). The mean solar global radiation, 1001 kWh m^{-2}, measured in Denmark between 1990 and 2010 (Skalik and Skalikova, 2019) and the mean wavelength of sunlight between 280 and 700 nm, were used to calculate the solar equivalence. The details of the calculations can be found in the supplementary material (S1). The solar equivalence of 7, 14, 21 and 28 days of UV-C exposure corresponded to 25, 50, 76 and 101 days based on the number of emitted photons. We evaluated the weathering of the paint materials from their infrared (IR) spectra collected by ATR-FTIR using a Cary 630 FTIR Spectrometer from Agilent Technologies with a germanium internal reflectance element. We collected 20 spectra for each non-exposed paint flake and 15 for each exposed paint flake after UV exposure every seven days (4000-650 cm^{-1}, 4 cm^{-1} spectral resolution, 64 co-added scans). The deformed shape and brittle nature of the exposed flakes hindered further collection of spectra. Based on an initial trial to compare the rates of weathering on paints, microparticles of the paint mix were weathered for 14 days while the particles of Alusafe for 7days and were mixed daily to ensure homogeneity of UV-exposure.

2.3. Identification of paint spectra

We corrected the collected IR spectra of non-exposed and UV-exposed paints for interferences giving rise to baseline slope and noise. The number of manipulations was minimal to optimise signal enhancement without distorting the spectra (Rinnan et al., 2009). We normalised the spectra by dividing all absorbance

Table 1
Properties of the investigated marine antifouling paints.

Paint		Manufacturer	Colour	Metal compounds
Cruiser Uno EU	YBB800	International	dove white	ZnO, Cu_2O
Eroding Antifouling	NAU703	Nautical	navy	ZnO, Cu_2O
Hard Racing Xtra	71420	Hempel	black	ZnO, Cu_2O
Seajet	033 Shogun	Jotun	red	ZnO, Cu_2O, Zineb
Yachting	Non-Stop 7520	Jotun	red	ZnO, Cu_2O
Alusafe	7120D	Hempel	blue	ZnO, zinc-pyrithione

values in a spectrum by the highest absorbance value to set a common intensity scale (Smith, 1999, 2011). We applied extended multiplicative scatter correction (EMSC) to reduce noise and baseline slope from scatter. The method handles both interferences simultaneously while maintaining the different absorbances by organic and inorganic components in the paint spectra (Rinnan et al., 2009; Martens and Starks, 1991; Liland et al., 2016). We applied baseline correction using the peak filling method (Liland, 2015), standard normal variate (SNV) scatter correction (Rinnan et al., 2009) and 9-point smoothing applying the Savitzky-Golay algorithm for the sole purpose of visualising spectra.

We compared the spectra from the Score described in Primpke et al. (2020) used for the automated identification of microplastic particles in infrared maps (Primpke et al., 2017, 2019, 2020; Liu et al., 2019; Vianello et al., 2019). The calculations employ the Pearson correlation coefficients between the raw, first and second derivatives of a reference and sample spectrum. We calculated the first and second derivatives of the pre-processed spectra using the Savitzky-Golay algorithm by fitting a second and third-order polynomial, respectively, with a five-point smoothing window-size (Rinnan et al., 2009; Kucheryavskiy, 2020). The Score can take values between 0 and 1. The highest numbers indicate a perfect fit between the reference and sample spectra. The details of the calculations are summarised in the supplementary material (S2).

We used RStudio v.1.2.5 (RStudio Team, 2019) and the packages EMSC (LilandKristian, 2020) for extended multiplicative scatter correction, baseline (Liland et al., 2010) for baseline correction and mdatools (Kucheryavskiy, 2020) for calculating derivatives and applying SNV. The Pearson correlation coefficients were calculated with Primer-e v.7 (PRIMER-E Ltd., UK).

2.4. Particle size analysis

We used FlowCam® 8000 Series Dynamic Imaging Particle Analyzer (Fluid Imaging Technologies, Inc., Scarborough, MA, USA) and Stereo Discovery v.8 stereomicroscope (Zeiss GmbH, Oberkochen, Germany) to characterise the particle sizes of paint microparticles before and after weathering. The nominal lower and upper sizes of both paint mix and Alusafe particles were 20 and 500 μm, respectively, based on the mesh size of the sieves applied for size fractionation during sample preparation. Nevertheless, smaller particles could be expected in both paint mix and Alusafe samples exposed to UV-C radiation as UV-exposure can cause particle fragmentation. The FlowCam® was equipped with a 4X objective and the corresponding flow cell allowed the acquisition of morphological data of particles between 12 and 300 μm as stated by the manufacturer. The instrument was used with the factory-set calibration and only the autofocus of the objective was adjusted manually before measurements. Red polystyrene beads, 100 μm in diameter (Sigma-Aldrich, product no. 56969) were used to ensure proper alignment and autofocus of the objective as recommended by the manufacturer. The “Best Focus Image” automatic autofocus algorithm was selected to enable good image quality of heterogeneous particles. Demineralised water (1 mL) pre-filtered through 1.2 μm cellulose acetate filter mesh was added to the funnel inserted in the sample introduction port followed by a few drops of the microbead suspension to perform the autofocus calibration.

Next, the paint microparticle samples were prepared for analysis. Particles were suspended in Milli-Q water containing a few drops of Tween 20 to reduce the surface tension of the hydrophobic particles and facilitate their homogenous dispersion in the liquid. The prepared particle suspension was gradually added to the FlowCam® system. The flow- and the auto image rates were set to achieve approx. 70% efficiency, thereby minimising multi-imaging of particles. Since particles larger than 300 μm could not enter the flow cell, we collected them by backflushing the cell after each measurement and analysed the collected particles using the stereomicroscope and the software ImageJ 1.53a. We characterised the particles from their surface areas.

2.5. Metal release from paint microparticles

To simulate metal leaching from paint microparticles in freshwater conditions, we used ISO 8692:2004 standard (International Organization for Standardization) algae growth media as the leaching solution (S3). Applying an artificial medium was preferred to natural water to minimise possible interferences and side-reactions from particulate matter, chelating agents and others. The artificial leaching media facilitated the evaluation of leaching mechanisms under freshwater conditions. All glassware was meticulously flushed with 1% nitric acid before the experiments to remove possible remaining traces of metals from the glassware, thus prevent contamination. One hundred milligrams of the 14-day-exposed paint mix and 7-day-exposed Alusafe microparticles were leached in 10 mL media separately in 50 mL glass conical flasks covered with Parafilm, agitated in the dark at 200 rpm, at 20 °C on an orbital shaker. Such a liquid to solid ratio was deemed suitable for this study because it prevented overcrowding the sample with microparticles while ensuring detectable concentrations of the inorganic compounds of interest. Microparticles were leached for 1, 6, 24, 48, 72 and 168 h. Separate sets of triplicate samples were prepared for each of the leaching periods. The particle suspensions were filtered through 0.45 μm nylon syringe filters into individual 10 mL centrifuge tubes to remove microparticles after 1, 6, 24, 48, 72 and 168 h.

Controls were prepared in triplicates corresponding to each leaching period with leaching medium alone, agitated and filtered under the same conditions as the microparticles. The filtered samples were acidified by adding concentrated nitric acid. We applied microwave-assisted digestion (Anton Paar Multiwave 7000, Graz, Austria) to both non-exposed and UV-exposed paint mix and Alusafe microparticles to determine their total metal content. The digesting solution comprised three parts PlasmaPure nitric acid (67–69%) and one part Suprapur® hydrogen peroxide (30%) and was added to 10 mg particles in 30 mL PTFE tubes in triplicate. During the 30-min-long ramp phase of the extraction procedure the temperature reached 250 °C, the pressure 130 bars and the power 900 W. The ramp phase was followed by an isothermal period of 15 min after which the samples were cooled to 80 °C with a pressure release rate of 10 bar min^{-1} for additional 25 min. The resulting liquid from the digested particles and the acidified particle leachates were analysed on a Thermo iCap 6000 ICP-OES (Thermo Fisher Scientific, USA) using yttrium as internal standard (IS). The instrument power was 1.15 kW and the samples were introduced through a glass concentric nebuliser. The plasma viewing configuration was axial at resonance lines of 396.1 for aluminium, 214.4 nm for cadmium, 267.7 nm for chromium, 324.7 nm for copper, 220.3 nm for lead, 180.7 for sulphur and 202.5 nm for zinc. A mixture of metal standards was used for calibration between 10 and 1000 μg L^{-1}. The limit of detection and quantification of each element of interest were determined from the standard calibration curves and are found in the supplementary material (S4).

3. Results

3.1. ATR-FTIR analysis of paints

3.1.1. Spectra of paints

Fig. 1 shows the average of the corrected 20 spectra of each paint

collected before UV-C exposure as well as the average of 15 spectra of the paints collected after each exposure interval. High-resolution versions of the spectra can be found in the supplementary material (S5). The spectral bands from non-exposed paints derived mainly from the paint binder. The detailed band assignments are summarised in Table 2. The acidic C═O and metal-carboxylate groups are associated with rosin, a common component of the binder in controlled depletion paint systems (Yebra et al., 2004, 2005). Rosin is a natural material derived from conifer trees, mainly consisting of resin-acids that are monocarboxylic acids with various diterpene skeletons (Yebra et al., 2004; Kugler et al., 2019). Although natural polymers are not usually considered microplastics, modified natural biopolymers are included in this pollutant group (Andrady, 2017; Verschoor, 2015). Therefore, rosin-based antifouling paint formulations are classified as microplastics, as rosin is often modified for the specific application (Yebra et al., 2004; Kugler et al., 2019). Rosin was the main constituent of the binder of Cruiser, Nautical and Seajet paints, while the binder of Alusafe, Racing and Yachting was made of an acrylate-rosin blend indicated by the presence of the carbonyl (C═O) stretching band of acrylate groups.

The paint spectra consisted predominantly of bands present in the binder structure, though inorganic components and metal complexes were also identified. Azémard et al. (2014) and Scalarone et al. (2002) reported similar changes of rosin upon accelerated weathering, as shown in Fig. 1. The authors attribute the observed growth of the broad band between 3500 and 3200 cm^{-1} to the formation of hydroxyl groups due to photooxidation of the unsaturated groups of the resin acids. While bands attributed to the carbonyl groups increased in intensity, probably because of the newly formed oxidation products that included ketones and lactones, bands attributed to methyl and methylene groups decreased in intensity possibly due to the loss of volatile compounds and degradation products (Azémard et al., 2014; Scalarone et al., 2002).

3.1.2. Quantifying changes in ATR-FTIR spectra

Fig. 2 illustrates that UV-induced alterations in the spectra decreased the Score of Alusafe, Nautical, Racing and Yachting paints compared with reference spectra. Seven days of UV-exposure resulted in the largest decrease, while further exposure only slightly lowered the index values used to characterise microplastics in environmental samples. Applying EMSC as a pre-processing step improved the correlation score measurably, possibly due to a decrease in spectral noise. Furthermore, the correlation of spectra of UV-exposed materials yielded higher Score values than the correlation between the UV-exposed and non-exposed variants of each paint (S6). Nevertheless, spectral changes did not influence the identification of Cruiser and Seajet paints significantly.

3.2. Particle size distribution

Fig. 3 illustrates the distribution of the measured area of the non-exposed and UV-exposed Alusafe and paint mix microparticles on a logarithmic scale. Smaller particles were more abundant among the exposed Alusafe particles than the non-exposed variant reflected in lower mean particle area. Nevertheless, the paint mix particles exhibited different size characteristics to the Alusafe particles. Though the non-exposed and exposed paint mix particles' size distributions appear similar, the mean area of the UV-exposed paint mix particles was significantly greater than the non-exposed particles (Kolmogorov-Smirnov test, $p = 2.2 \cdot 10^{-16}$) indicating that larger particles were more abundant in the exposed particles.

3.3. Leaching of inorganic elements from antifouling paint microparticles

The Alusafe microparticles contained zinc at the highest concentration (34%) and aluminium (1.7%), while cadmium, chromium, copper and lead were present in low concentrations (<1%). Copper and zinc represented the largest mass fraction in the paint mix microparticles (26% and 10%, respectively). The paint mix particles contained cadmium, chromium, aluminium and lead in low concentrations (<1%). Besides, both paint mix and Alusafe microparticle samples contained a substantial amount of sulphur (S7). Fig. 4 shows the release of inorganic elements from non-exposed and 14-day-exposed paint mix and 7-day-exposed Alusafe microparticles throughout the experiment. The displayed concentrations are the mean values of triplicate determinations after correction for their

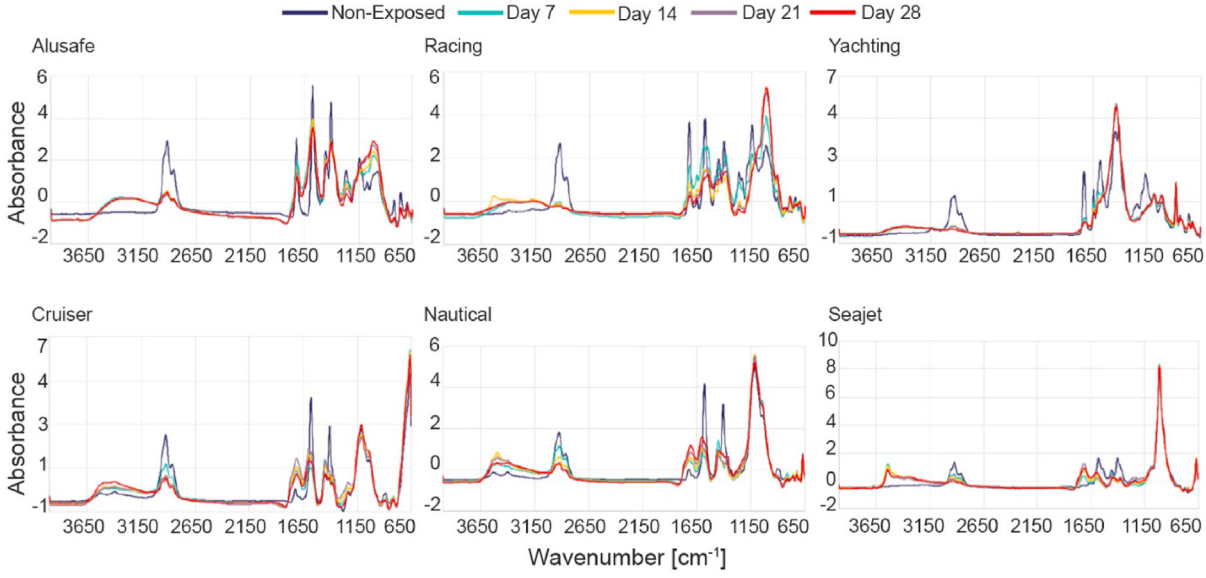

Fig. 1. Average of 20 ATR-FTIR spectra of the non-exposed paints and average of 15 spectra collected after UV-C exposure. All spectra were normalised, then baseline corrected, standard normal variate scatter corrected and smoothed with a nine-point window using the Savitzky-Golay algorithm.

Table 2
Assignment of the infrared absorption bands of the average spectra of all paints based on * Smith (1999), ***van der Weerd* et al. (van der Weerd et al., 2005) *and* ***Singh and Turner (2009a).

Wavenumber [cm^{-1}]	Group vibration	Origin
3529, 3545, 3390	Overtone of silicate*	Pigment
3500–3200	OH*	Oxidation
3139	Unsaturated C–C bond*	Binder
2924	Methylene asymmetric C–H stretch*	Binder
2864	Methyl symmetric C–H stretch*	Binder
1719/1724	Acrylic C=O stretch*	Binder
1700	Carboxylic acid C=O stretch*	Binder/Oxidation
1654	C=C**	Binder
1578, 1593	Metal carboxylate asymmetric COO stretch*	Binder
1448, 1457	C–H scissoring of methylene group*	Binder
1406	Metal carboxylate, symmetric COO stretch*	Binder
1376	C–H symmetric deformation in CH3 group*	Binder
1360	C–CH3 asymmetric bend*	Binder
1266, 1240, 1146	C–C–O, C–C–C, O–C–C stretches from acrylate*	Binder
1235	C–O*	Binder
1115	Silicate**	Pigment
1012	Silicate, Si–O–Si asymmetric stretching*	Pigment
1105	Ferric oxide**	Pigment
820	Zn-pyrithione***	Metal-complex
668	Ferric oxide*	Pigment

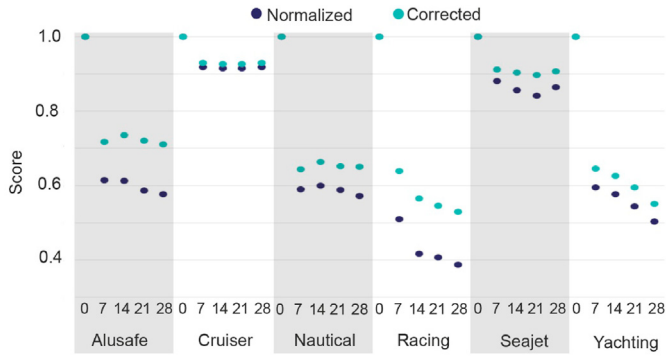

Fig. 2. The Score as a measure of similarity between spectra was calculated from the Pearson correlation of the average non-exposed spectra and those collected after UV-exposure. The Score takes the value of 1 in case of a perfect similarity at time 0. Normalised and scatter-corrected average spectra and their first and second derivatives were employed in the calculations.

respective mean control values. The error bars represent the standard deviation around the mean. The fractions of leached elements after 168 h are annotated in the figures and show greater mobility in the exposed than in the non-exposed particles. Not all elements extracted from the particles by digestion could be detected in the leachates, which can be related to their differing mobilities in the paint matrix. For instance, aluminium was detected in neither the non-exposed nor the exposed paint mix leachates during the experiment. Similarly, chromium was not detected in any Alusafe and paint mix leachates, while lead could only be detected in the UV-exposed paint mix particles' leachates. A higher initial release occurred for most of the inorganic elements from UV-exposed particles than from their non-exposed equivalents. The high initial leaching from UV-exposed paint mix and Alusafe particles was followed by slight concentration increase. However, the concentration of most elements in the aqueous phase showed a steady increase throughout the experiment in case of the non-exposed particles, exemplified by zinc from non-exposed paint mix particles and cadmium from non-exposed Alusafe particles. Furthermore, the aqueous zinc concentration in the leachates of both non-exposed and UV-exposed Alusafe particles decreased over time. The pH values of particle leachates were generally lower than the corresponding controls, though the difference was more notable in leachates from UV-exposed particles (S8).

4. Discussion

4.1. Characterisation of paint microparticles

ATR-FTIR spectra of paints revealed that their binders comprised rosin or rosin-acrylate blends. The silicates and ferric oxide identified in the rosin-based paints are usually added to improve the coating's mechanical properties and adjust their polishing rates (Yebra et al., 2005; van der Weerd et al., 2005; Yebra and Weinell, 2009). The addition of a water-insoluble co-binder to rosin, for example, in a rosin-acrylate blend, can also optimise the material's hydrophobicity and polishing rate (Yebra et al., 2004). The carboxyl group in resin acids can form metal-carboxylates, known as resinates, with the metals present in paints as biocides, pigments, or other additives (Yebra et al., 2005).

4.2. UV-C induced chemical changes in the material

Exterior coatings are exposed to environmental impacts, such as sunlight, fluctuating temperature, humidity and atmospheric pollutants (Kockott, 1989; Kämpf et al., 1991). These weathering factors not only deteriorate the aesthetic properties of the coatings but disrupt their structures, thereby changing their mechanical properties and performance over time (Kockott, 1989). Therefore, the weathering resistance of coatings and other polymers has significant practical importance (Rabek, 1990; Kockott, 1989). Weathering tests of stable commercial materials under natural conditions can take an inconveniently long time due to the added stabilising compounds that prolong the materials' service life (Sommer et al., 1991; Wypych, 2018). The advantage of accelerated tests, such as the one applied in the present study that employed UV-C radiation, lies in substantial time reduction and reproducible, controlled environment for experiments (Sommer et al., 1991; Wypych, 2018). However, the results of an accelerated test cannot predict the outdoor weathering behaviour of the material unless the degradation mechanisms are identical under both artificial and natural conditions (Sommer et al., 1991; Wypych, 2018). As a result, the UV-C radiation employed to weather the paint particles cannot be directly translated to natural sunlight exposure because UV-C is

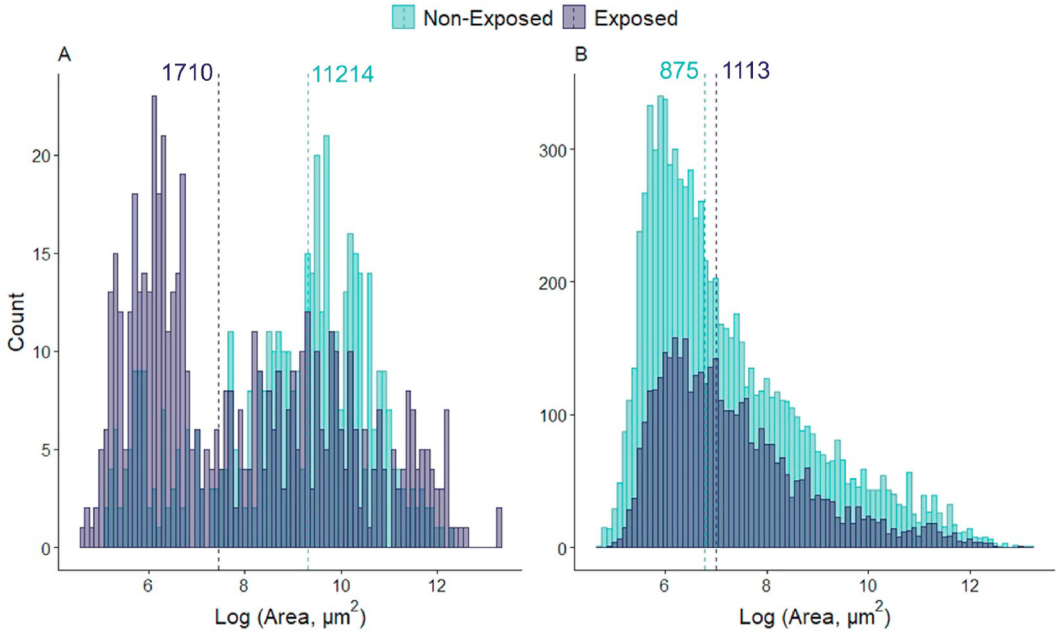

Fig. 3. Distribution of the area of non-exposed and 7-day-exposed Alusafe (A) and non-exposed and 14-day-exposed paint mix (B) particles on a logarithmic scale. The size of the bins was 0.1. The median area of the different samples is annotated.

filtered out by the atmosphere and is not a constituent of natural solar radiation reaching the Earth's surface (Brennan and Fedor, 1987). Furthermore, UV-C can break chemical bonds that natural sunlight would not be able to, due to the former's higher quantum energy, potentially inducing different degradation mechanisms (Kockott, 1989; Brennan and Fedor, 1987; Saunders, 1988). Despite these caveats, UV-C radiation induced the oxidation of polymers and deteriorated the structure of the material. Since information on the degradability of the investigated materials was unavailable at the start of this study, accelerated weathering produced degraded material in a time-efficient manner.

The observed alterations induced by UV-C exposure represented those of the material's upper layers as spectra were collected from the surface by ATR-FTIR spectroscopy. The germanium internal reflection element has a particularly shallow depth of penetration, focusing examination on the upper few microns of a surface and not on the bulk of the material (Smith, 2011). The similarity index's values, the Score of Alusafe, Racing, Yachting and Nautical decreased considerably after seven days of UV-exposure, while further subtle alterations in the material slightly affected the spectral similarity between the exposed and non-exposed paints. This observation corresponds with that of Azérmand et al. (Azémard et al., 2014) and Scalarone et al. (2002), describing the most notable changes in the infrared spectra of rosin at the early stage of their weathering tests.

Although the data presented in the current research originates in particles of uniform materials exposed to a single impact in a controlled environment and the resulting spectra had a high signal to noise ratio, we calculated correlation scores below, e.g., 0.4 of the Racing paint. These results demonstrate that changes in the material could affect the automatic identification of the paint particles. Microplastics (MPs) in the environment are exposed to various abiotic and biotic impacts that can cause degradation and oxidation, possibly altering their FTIR spectra (Andrady, 2011b, 2017; Brandon et al., 2016; Tidjani, 2000; Cai et al., 2018). Unknown spectra are commonly compared with spectra collected from the pristine, undegraded form of known materials (Smith, 1999; Lenz et al., 2015). This practice potentially increases the number of false negatives if the differences exceed a certain degree (Lenz et al., 2015). In addition, differing acquisition modes of the reference and unknown spectra can result in discrepant spectra further hindering identification (Harrison et al., 2012).

Our findings suggest that including spectra of weathered material could improve identification because the Score had higher values when spectra of weathered material were compared with each other than with pristine material. Scatter-corrected spectra yielded the highest Score values between non-exposed and UV-exposed spectra, suggesting that pre-processing steps could also increase the certainty of identification (Solheim et al., 2019). It is plausible that scatter-correction has a larger influence on spectra collected using imaging systems where the intrinsic scatter effects are stronger, compared with ATR-FTIR spectroscopy (Harrison et al., 2012; Simon et al., 2018; Vianello et al., 2013). Nevertheless, changes in the spectra of Cruiser and Seajet paints did not decrease the Scores because the bands with the highest intensities derived from inorganic components were stable during exposure.

4.3. The effect of UV-induced changes on particle properties

The study by Luo et al. (2020) supports our findings that a larger fraction of the inorganic elements was released from microparticles exposed to accelerated weathering. The physical and chemical changes induced by UV-C exposure in the paint microparticles may be attributed to the increased metal mobility since constant experimental conditions throughout the leaching of exposed and non-exposed particles did not change the solubility of inorganic components. Infrared spectroscopy of the paints revealed that UV-exposure likely impaired the binder's structure due to the loss of volatile compounds and degradation products and generated hydrophilic, reactive groups. The compromised integrity and increased reactivity resulted in enhanced water intrusion into the bulk of the binder, possibly accelerating its erosion, causing greater metal dissolution. The hydrolysis of a large amount of released zinc (equation (2) (Hanzawa et al., 1997)), copper, aluminium and

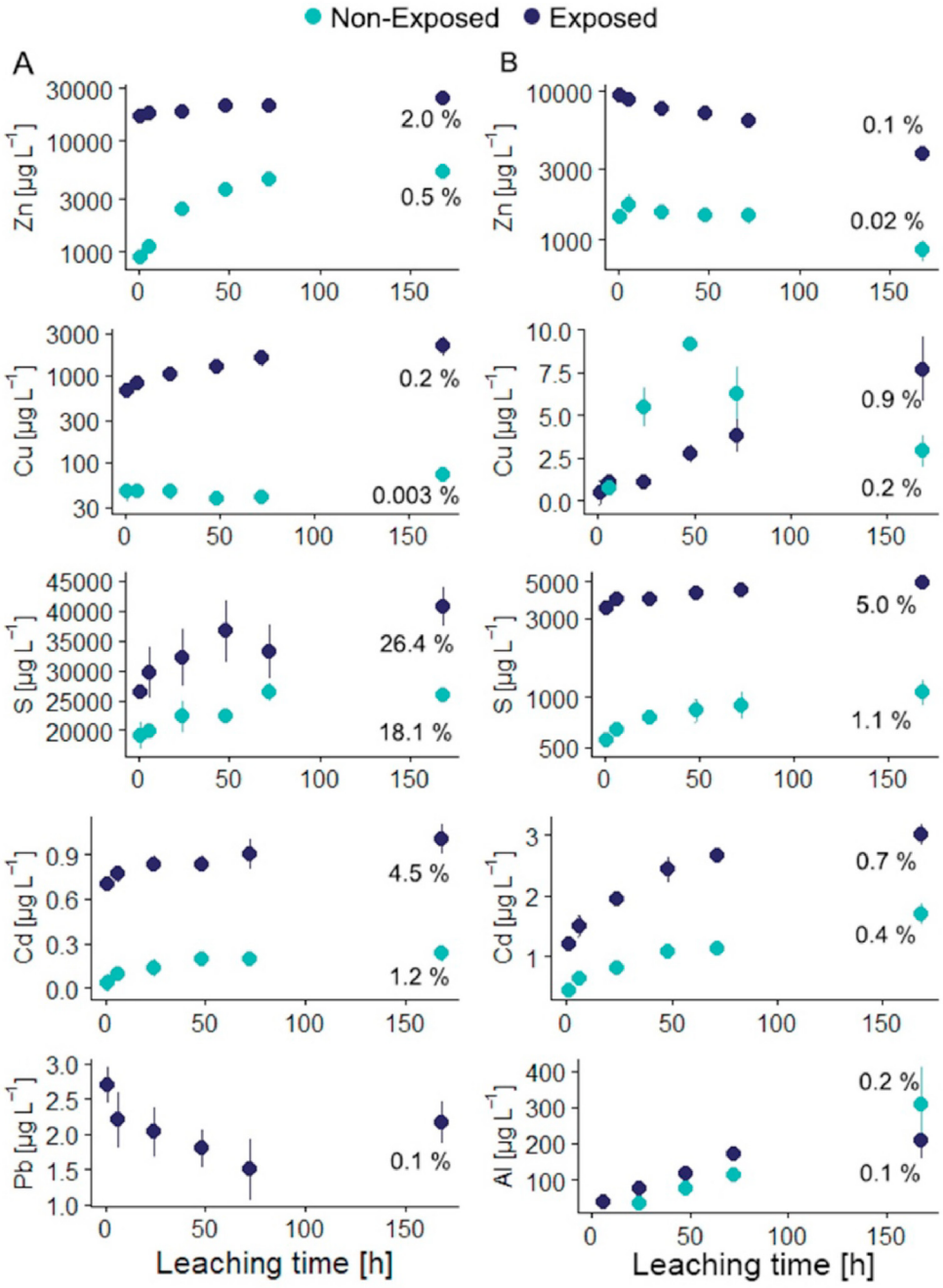

Fig. 4. The concentration of elements measured in the leachates of non-exposed and UV-exposed paint mix (column A) and Alusafe (column B) microparticles throughout the experiment. The fractions of the total concentration that leached after 168 h are shown on the right-hand sides.

cadmium (Gayer and Haas, 1960; Frink and Peech, 1963) may have contributed to the observed pH decrease. The acidic pH can promote the dissolution of metals directly by, e.g., equation (3) (Yebra et al., 2006) and 4 (a Palmer and Benezeth, 2008) and by reacting with the binder (Vallee-Rehel et al., 1998).

$$Zn^{2+} + 2H_2O = Zn(OH)_2 + 2H^+ \quad (2)$$

$$ZnO + 2H^+ = Zn^{2+} + H_2O \quad (3)$$

$$½\ Cu_2O + H^+ = Cu^+ + ½\ H_2O \quad (4)$$

Reduction in physical properties, including particle size, may also account for differing metal release. Smaller particles have higher active surface areas and a greater potential for leaching. Since the UV-exposed Alusafe microparticles were smaller than the non-exposed material, their dimensions could account for higher metal leaching from the exposed particles. Nevertheless, Singh and Turner (2009b) found no significant difference in the metal release from spent antifouling paint particles of different size ranges. Several authors linked the insensitivity of metal release to particle size to various interactions between the released metals and leached paint components that can affect their aqueous concentration (Singh and Turner, 2009b; Albrecht et al., 2011; Holmes and Turner, 2009; Jessop and Turner, 2011; Sandberg et al., 2007). Such interactions, including re-sorption to the particle surface,

precipitation, chelation, are indicated by the decrease in the aqueous zinc concentration in the case of both non-exposed and UV-exposed Alusafe particles. Furthermore, the particle size data of the paint mix particles do not explain larger leaching rates of metals from the UV-exposed paint mix particles than from the non-exposed sample because the mean area of the exposed particles was larger than of the non-exposed paint mix particles. This observation is counterintuitive because UV-exposure causes embrittlement of particles that fragment further to smaller particles (Andrady, 2017). It is possible that UV-exposed paint mix microparticles fragmented to a size below the detection limit of the particle imaging instrument's cut-off of 12 μm. To summarise, it is difficult to evaluate the role of particle size in metal release based on these results. Further investigation is required, perhaps by applying different settings of the FlowCam® that would allow examination of small particles or comparing leaching experiments carried out with microparticles of different size ranges.

Our results suggest that UV-C induced changes in the chemical makeup of paint microparticles because the enhanced reactivity of the binder and its impaired structure increased metal release. It furthermore changed the chemical environment of the leaching media, possibly by introducing organic paint components into the media and indirectly decreasing its pH through the hydrolysis of the released metals. The modified composition of the leaching media may have also affected metal leaching.

5. Conclusion

The present study highlights the importance of gathering knowledge about the fate of MPs in the environment. Our results showed that weathering can drastically change the chemical and physical properties of paint microparticles. These findings raise the question of the relevance of employing MPs of pristine material in impact studies. Furthermore, as MPs are usually exposed to a multitude of physicochemical factors rather than individual, single impacts, the effect of combining environmental conditions on the molecular composition of the material is of great importance. Our findings also suggest that an essential step towards improving the quality of MP identification is to include collections of ATR-FTIR spectra from weathered material in spectral databases. This addition is likely to improve the characterisation of weathered MPs that otherwise would be overlooked. Such a measure is likely to increase the significance of MP identification resulting in more robust data.

Credit author statement

Márta Simon: Conceptualisation, Methodology, Investigation, Writing – original draft, Alvise Vianello: Methodology, Writing – review & editing, Yvonne Shashoua: Writing – review & editing, Jes Vollertsen: Writing – review & editing, Supervision

Declaration of competing interest

The authors declare that they have no known competing financial interests or personal relationships that could have appeared to influence the work reported in this paper.

Acknowledgements

The study was part of the MarinePlastic centre- The Danish centre for research in marine plastic pollution funded by Velux Foundation, Denmark.

Appendix A. Supplementary data

Supplementary data to this article can be found online at https://doi.org/10.1016/j.chemosphere.2021.129749.

References

a Palmer, D., Benezeth, P., 2008. Solubility of copper oxides in water and steam. In: 14Th Int. Conf. Prop. Water Steam Kyoto.
Albrecht, T.W.J., Addai-Mensah, J., Fornasiero, D., 2011. Effect of pH , concentration and temperature on copper and zinc hydroxide formation/precipitation in solution. CHEMECA 2011 - "Engineering a Better World, pp. 1–10. http://arrow.unisa.edu.au:8081/1959.8/123424.
Andrady, A.L., 2011a. Microplastics in the marine environment. Mar. Pollut. Bull. 62, 1596–1605. https://doi.org/10.1016/j.marpolbul.2011.05.030.
Andrady, A.L., 2011b. Microplastics in the marine environment. Mar. Pollut. Bull. 62, 1596–1605. https://doi.org/10.1016/j.marpolbul.2011.05.030.
Andrady, A.L., 2017. The plastic in microplastics: a review. Mar. Pollut. Bull. 119, 12–22. https://doi.org/10.1016/j.marpolbul.2017.01.082.
ECHA, 2019. ECHA Annex XV Restriction Report 2019. Annankatu 18, PO BOX 400, FI-00121. Finland., Helsinki, p. 146. https://echa.europa.eu/documents/10162/05bd96e3-b969-0a7c-c6d0-441182893720.
Azémard, C., Vieillescazes, C., Ménager, M., 2014. Effect of photodegradation on the identification of natural varnishes by FT-IR spectroscopy. Microchem. J. 112, 137–149. https://doi.org/10.1016/j.microc.2013.09.020.
Bejgarn, S., MacLeod, M., Bogdal, C., Breitholtz, M., 2015. Toxicity of leachate from weathering plastics: an exploratory screening study with Nitocra spinipes. Chemosphere 132, 114–119. https://doi.org/10.1016/j.chemosphere.2015.03.010.
Brandon, J., Goldstein, M., Ohman, M.D., 2016. Long-term aging and degradation of microplastic particles: comparing in situ oceanic and experimental weathering patterns. Mar. Pollut. Bull. 110, 299–308. https://doi.org/10.1016/j.marpolbul.2016.06.048.
Brennan, P., Fedor, C., 1987. Sunlight, Uv and Accelerated Weathering 55, 198–203. https://doi.org/10.1016/0306-3747(88)90432-0.
Browne, M.A., Galloway, T.S., Thompson, R.C., 2007. MICROPLASTIC—an emerging contaminant OF potential concern? Integr. Environ. Assess. Manag. preprint 1. https://doi.org/10.1897/ieam_2008-022.1.
Cai, L., Wang, J., Peng, J., Wu, Z., Tan, X., 2018. Observation of the degradation of three types of plastic pellets exposed to UV irradiation in three different environments. Sci. Total Environ. 628–629, 740–747. https://doi.org/10.1016/j.scitotenv.2018.02.079.
Decelis, R., Vella, A.J., 2007. Contamination of outdoor settled dust by butyltins in Malta. Appl. Organomet. Chem. 21, 239–245. https://doi.org/10.1002/aoc.1207.
Frink, C.R., Peech, M., 1963. Hydrolysis of the aluminum ion in dilute aqueous solutions. Inorg. Chem. 2, 473–478. https://doi.org/10.1021/ic50007a011.
Gayer, K.H., Haas, R.M., 1960. Hydrolysis of cadmium chloride at 25°. J. Phys. Chem. 64, 1764–1766. https://doi.org/10.1021/j100840a505.
Hahladakis, J.N., Velis, C.A., Weber, R., Iacovidou, E., Purnell, P., 2018. An overview of chemical additives present in plastics: migration, release, fate and environmental impact during their use, disposal and recycling. J. Hazard Mater. 344, 179–199. https://doi.org/10.1016/j.jhazmat.2017.10.014.
Hammer, J., Kraak, M.H.S., Parsons, J.R., 2012. Plastics in the Marine Environment: the Dark Side of a Modern Gift. https://doi.org/10.1007/978-1-4614-3414-6.
Hanzawa, Y., Hiroishi, D., Matsuura, C., Ishigure, K., Nagao, M., Haginuma, M., 1997. Hydrolysis of zinc ion and solubility of zinc oxide in high-temperature aqueous systems. Nucl. Sci. Eng. 127, 292–299. https://doi.org/10.13182/NSE97-03.
Harrison, J.P., Ojeda, J.J., Romero-González, M.E., 2012. The applicability of reflectance micro-Fourier-transform infrared spectroscopy for the detection of synthetic microplastics in marine sediments. Sci. Total Environ. 416, 455–463. https://doi.org/10.1016/j.scitotenv.2011.11.078.
Hartmann, N.B., Hüffer, T., Thompson, R.C., Hassellöv, M., Verschoor, A., Daugaard, A.E., Rist, S., Karlsson, T., Brennholt, N., Cole, M., Herrling, M.P., Hess, M.C., Ivleva, N.P., Lusher, A.L., Wagner, M., 2019. Are we speaking the same language? Recommendations for a definition and categorization framework for plastic debris. Environ. Sci. Technol. 53, 1039–1047. https://doi.org/10.1021/acs.est.8b05297.
Hermabessiere, L., Dehaut, A., Paul-Pont, I., Lacroix, C., Jezequel, R., Soudant, P., Duflos, G., 2017. Occurrence and effects of plastic additives on marine environments and organisms: a review. Chemosphere 182, 781–793. https://doi.org/10.1016/j.chemosphere.2017.05.096.
Holmes, L., Turner, A., 2009. Leaching of hydrophobic Cu and Zn from discarded marine antifouling paint residues: evidence for transchelation of metal pyrithiones. Environ. Pollut. 157, 3440–3444. https://doi.org/10.1016/j.envpol.2009.06.018.
International Organization for Standardization [ISO], Water Quality - Fresh Water Algal Growth Inhibition Test with Unicellular Green Algae., (n.d.) 21.
Jartun, M., Pettersen, A., 2010. Contaminants in urban runoff to Norwegian fjords. J. Soils Sediments 10, 155–161. https://doi.org/10.1007/s11368-009-0181-y.
Jessop, A., Turner, A., 2011. Leaching of Cu and Zn from discarded boat paint particles into tap water and rain water. Chemosphere 83, 1575–1580. https://doi.org/10.1016/j.chemosphere.2011.01.021.
Kämpf, G., Sommer, K., Zirngiebl, E., 1991. Studies in accelerated weathering. Part I. Determination of the activation spectrum of photodegradation in polymers.

Prog. Org. Coating 19, 69–77. https://doi.org/10.1016/0033-0655(91)80011-7.
Kockott, D., 1989. Natural and artificial weathering of polymers. Polym. Degrad. Stabil. 25, 181–208. https://doi.org/10.1016/S0141-3910(89)81007-9.
Kucheryavskiy, S., 2020. Mdatools – R package for chemometrics. Chemometr. Intell. Lab. Syst. 198, 103937. https://doi.org/10.1016/j.chemolab.2020.103937.
Kugler, S., Ossowicz, P., Malarczyk-Matusiak, K., Wierzbicka, E., 2019. Advances in rosin-based chemicals: the latest recipes, applications and future trends. Molecules 24. https://doi.org/10.3390/molecules24091651.
Lenz, R., Enders, K., Stedmon, C.A., MacKenzie, D.M.A., Nielsen, T.G., 2015. A critical assessment of visual identification of marine microplastic using Raman spectroscopy for analysis improvement. Mar. Pollut. Bull. 100, 82–91. https://doi.org/10.1016/j.marpolbul.2015.09.026.
Liland, K.H., 2015. 4S Peak Filling - baseline estimation by iterative mean suppression. Methods 2, 135–140. https://doi.org/10.1016/j.mex.2015.02.009.
Liland, K.H., Almøy, T., Mevik, B.H., 2010. Optimal choice of baseline correction for multivariate calibration of spectra. Appl. Spectrosc. 64, 1007–1016. https://doi.org/10.1366/000370210792434350.
Liland, K.H., Kohler, A., Afseth, N.K., 2016. Model-based pre-processing in Raman spectroscopy of biological samples. J. Raman Spectrosc. 47, 643–650. https://doi.org/10.1002/jrs.4886.
Liland, Hovde, Kristian, U.G. Indahl, 2020. Package ' EMSC. https://CRAN.R-project.org/package=EMSC.
Lithner, D., Larsson, A., Dave, G., 2011. Environmental and health hazard ranking and assessment of plastic polymers based on chemical composition. Sci. Total Environ. 409, 3309–3324. https://doi.org/10.1016/j.scitotenv.2011.04.038.
Liu, F., Olesen, K.B., Borregaard, A.R., Vollertsen, J., 2019. Microplastics in urban and highway stormwater retention ponds. Sci. Total Environ. 671, 992–1000. https://doi.org/10.1016/j.scitotenv.2019.03.416.
Luo, H., Li, Y., Zhao, Y., Xiang, Y., He, D., Pan, X., 2020. Effects of accelerated aging on characteristics , leaching , and toxicity of commercial lead chromate pigmented microplastics. Environ. Pollut. 257 https://doi.org/10.1016/j.envpol.2019.113475.
Martens, H., Starks, E., 1991. Extended multiplicative signal correction and spectral interference subtraction: new preprocessing methods for near infrared spectroscopy. J. Pharmaceut. Biomed. Anal. 9, 625–635. https://doi.org/10.1002/bate.200810020.
Primpke, S., Lorenz, C., Rascher-Friesenhausen, R., Gerdts, G., 2017. An automated approach for microplastics analysis using focal plane array (FPA) FTIR microscopy and image analysis. Anal. Methods. 9, 1499–1511. https://doi.org/10.1039/c6ay02476a.
Primpke, S., Dias, P.A., Gerdts, G., 2019. Automated identification and quantification of microfibres and microplastics. Anal. Methods. 11, 2138–2147. https://doi.org/10.1039/c9ay00126c.
Primpke, S., Cross, R.K., Mintenig, S.M., Simon, M., Vianello, A., Gerdts, G., Vollertsen, J., 2020. EXPRESS: toward the Systematic Identification of Microplastics in the Environment: Evaluation of a New Independent Software Tool (siMPle) for Spectroscopic Analysis. https://doi.org/10.1177/0003702820917760.
Rabek, J.F., 1990. Photostabilization of Polymers: Principles and Application. Elsevier Science Publishers Ltd, ISBN 978-94-010-6821-5. https://doi.org/10.1007/978-94-009-0747-8.
Rinnan, Å., van den Berg, F., Engelsen, S.B., 2009. Review of the most common pre-processing techniques for near-infrared spectra. TrAC Trends Anal. Chem. (Reference Ed.) 28, 1201–1222. https://doi.org/10.1016/j.trac.2009.07.007.
Sandberg, J., Odenvall Wallinder, I., Leygraf, C., Virta, M., 2007. Release and chemical speciation of copper from anti-fouling paints with different active copper compounds in artificial seawater. Mater. Corros. 58, 165–172. https://doi.org/10.1002/maco.200604002.
Saunders, K.J., 1988. Inorganic Polymer Chemistry. https://doi.org/10.1080/10601326708053916.
Scalarone, D., Lazzari, M., Chiantore, O., 2002. Ageing behaviour and pyrolytic characterisation of diterpenic resins used as art materials: colophony and Venice turpentine. J. Anal. Appl. Pyrolysis 64, 345–361. https://doi.org/10.1016/S0165-2370(02)00046-3.
Simon, M., van Alst, N., Vollertsen, J., 2018. Quantification of microplastic mass and removal rates at wastewater treatment plants applying Focal Plane Array (FPA)-based Fourier Transform Infrared (FT-IR) imaging. Water Res. 142 https://doi.org/10.1016/j.watres.2018.05.019.
Singh, N., Turner, A., 2009a. Trace metals in antifouling paint particles and their heterogeneous contamination of coastal sediments. Mar. Pollut. Bull. 58, 559–564. https://doi.org/10.1016/j.marpolbul.2008.11.014.
Singh, N., Turner, A., 2009b. Leaching of copper and zinc from spent antifouling paint particles. Environ. Pollut. 157, 371–376. https://doi.org/10.1016/j.envpol.2008.10.003.
Skalik, L., Skalikova, I., 2019. Long-term global radiation measurements in Denmark and Sweden. IOP Conf. Ser. Mater. Sci. Eng. 471 https://doi.org/10.1088/1757-899X/471/10/102004.
Smith, B.C., 1999. Infrared Spectral Interpretation: a Systemic Approach. CRC Press LLC, ISBN 0-8493-2463-7.
Smith, B.C., 2011. Fundamentals of Fourier Transform Infrared Spectroscopy, 2nd. ed. CRC press, Taylor & Francis Group, ISBN 978-1-4200-6929-7.
Solheim, J., Gunko, E., Petersen, D., Großerüschkamp, F., 2019. An open source code for Mie Extinction EMSC for infrared microscopy spectra of cells and tissues. J. Biophot. 10–16. https://doi.org/10.1002/jbio.201800415.
Sommer, A., Zirngiebl, E., Kahl, L., Schönfelder, M., 1991. Studies in accelerated weathering. Part II. Ultrafast weathering - a new method for evaluating the weather resistance of polymers. Prog. Org. Coating 19, 79–87. https://doi.org/10.1016/0033-0655(91)80012-8.
Tidjani, A., 2000. Comparison of formation of oxidation products during photo-oxidation of linear low density polyethylene under different natural and accelerated weathering conditions. Polym. Degrad. Stabil. 68, 465–469. https://doi.org/10.1016/S0141-3910(00)00039-2.
Turner, A., 2010. Marine pollution from antifouling paint particles. Mar. Pollut. Bull. 60, 159–171. https://doi.org/10.1016/j.marpolbul.2009.12.004.
Turner, A., Singh, N., Richards, J.P., 2009. Bioaccessibility of metals in soils and dusts contaminated by marine antifouling paint particles. Environ. Pollut. 157, 1526–1532. https://doi.org/10.1016/j.envpol.2009.01.008.
Vallee-Rehel, K., Langlois, V., Guerin, P., 1998. Contribution of pendant ester group hydrolysis to the erosion of acrylic polymers in binders aimed at organotin-free antifouling paints. J. Environ. Polym. Degrad. 6, 175–186. https://doi.org/10.1023/A:1021821614323.
van der Weerd, J., van Loon, A., Boon, J.J., 2005. FTIR studies of the effects of pigments on the aging of oil. Stud. Conserv. 50, 3–22. https://doi.org/10.1179/sic.2005.50.1.3.
Verschoor, A.J., 2015. Towards a Definition of Microplastics: Considerations for the Specification of Physico-Chemical Properties, RIVM Lett. Rep. 2015-0116. https://www.rivm.nl/bibliotheek/rapporten/2015-0116.pdf.
Vianello, A., Boldrin, A., Guerriero, P., Moschino, V., Rella, R., Sturaro, A., Da Ros, L., 2013. Estuarine , Coastal and Shelf Science Microplastic particles in sediments of Lagoon of Venice , Italy : first observations on occurrence , spatial patterns and identi fi cation. Estuar. Coast Shelf Sci. 130, 54–61.
Vianello, A., Jensen, R.L., Liu, L., Vollertsen, J., 2019. Simulating human exposure to indoor airborne microplastics using a Breathing Thermal Manikin. Sci. Rep. 9 https://doi.org/10.1038/s41598-019-45054-w.
Wypych, G., 2015. Principles of uv degradation. In: PVC Degrad. Stab., vols. 167–203. ChemTec Publishing, ISBN 9781895198850. https://doi.org/10.1016/b978-1-895198-85-0.50007-8.
Wypych, G., 2018. Artificial weathering versus natural exposure. Handb. Mater. Weather. 3, 241–257. https://doi.org/10.1016/b978-1-927885-31-4.50013-3.
Yebra, D.M., Weinell, C.E., 2009. Key Issues in the Formulation of Marine Antifouling Paints. Woodhead Publishing Limited. https://doi.org/10.1533/9781845696313.2.308.
Yebra, D.M., Kiil, S., Dam-Johansen, K., 2004. Antifouling technology - past, present and future steps towards efficient and environmentally friendly antifouling coatings. Prog. Org. Coating 50, 75–104. https://doi.org/10.1016/j.porgcoat.2003.06.001.
Yebra, D.M., Kiil, S., Dam-Johansen, K., Weinell, C., 2005. Reaction rate estimation of controlled-release antifouling paint binders: rosin-based systems. Prog. Org. Coating 53, 256–275. https://doi.org/10.1016/j.porgcoat.2005.03.008.
Yebra, D.M., Kiil, S., Weinell, C.E., Dam-Johansen, K., 2006. Dissolution rate measurements of sea water soluble pigments for antifouling paints: ZnO. Prog. Org. Coating 56, 327–337. https://doi.org/10.1016/j.porgcoat.2006.06.007.